Enhanced ferromagnetic interactions in electron doped $Nd_xSr_{2-x}FeMoO_6$ double perovskites

2004 J. Phys.: Condens. Matter 16 3173

(http://iopscience.iop.org/0953-8984/16/18/018)

INSTITUTE OF PHYSICS PUBLISHING JOURNAL OF PHYSICS: CONDENSED MATTER

J. Phys.: Condens. Matter **16** (2004) 3173–3182 PII: S0953-8984(04)74565-8

Enhanced ferromagnetic interactions in electron doped $Nd_xSr_{2-x}FeMoO_6$ double perovskites

D Rubi[1], C Frontera[1], J Nogués[2] and J Fontcuberta[1]

[1] Institut de Ciència de Materials de Barcelona (CSIC), Campus Universitat Autònoma de Barcelona, E-08193, Bellaterra, Catalunya, Spain
[2] Institució Catalana de Recerca i Estudis Avançats (ICREA) and Departament de Física, Universitat Autònoma de Barcelona, E-08193, Bellaterra, Catalunya, Spain

E-mail: fontcuberta@icmab.es

Received 9 January 2004
Published 23 April 2004
Online at stacks.iop.org/JPhysCM/16/3173
DOI: 10.1088/0953-8984/16/18/018

Abstract

We report on the structural, magnetic and magnetotransport effects promoted by Nd^{3+} substitution in $Nd_xSr_{2-x}FeMoO_6$. In spite of the fact that the ionic radius of Nd^{3+} is smaller than that of Sr^{2+}, the unit cell volume remains constant across the series. We also show that the incorporation of Nd^{3+} induces a substantial rising of the Curie temperature from $T_C = 400$ K for $x = 0$ to $T_C = 440$ K for $x = 0.6$. On the basis of the structural data we argue that this enhancement is due to the injection of itinerant carriers into the conduction band. Nd doping promotes the appearance of antisite (AS) defects in the Fe–Mo sublattice. It turns out that the concentration of AS is mainly controlled by the donor character of the substituting ions rather than by their ionic radii. Antisites are found to reduce the saturation magnetization *and* the magnetoresistance. This observation, which sharply contrasts with expectations based on electronic rigid band models, indicates that the half-metallic character of double perovskites may be unstable in the presence of antisites. This is in agreement with some recent proposals and the implications of these findings are discussed.

1. Introduction

Double perovskites of the type A_2FeMoO_6 (A = Sr, Ba) have been known for about 40 years. However, a recent work by Kobayashi [1] on Sr_2FeMoO_6 (SFMO) has stimulated renewed scientific interest, due to the claim that these oxides are half-metallic ferromagnets and display a large magnetoresistance below their Curie temperature (T_C), which is usually above room temperature. This feature suggests a great potential for use of such materials for the development of spintronics applications. Therefore, an intensive effort is being made to understand their structural, magnetic and transport properties. Of particular importance is

the development of strategies for raising T_C to higher temperatures, which would enlarge the working range of potential applications.

Recent studies on Sr_2FeMoO_6 [2] have suggested that the ferromagnetic (FM) ordering of localized Fe^{3+} ions (which belong to the 'spin up' valence band) is achieved through the mediation of delocalized 'spin down' conduction electrons. That is, ferromagnetism in SFMO is stabilized via an antiferromagnetic coupling between valence and conduction electrons. Furthermore, the mean-field model developed by Tovar *et al* [2] suggests that the intensity of FM coupling is directly related to the density of electrons at the Fermi level. Hence, the injection of electrons into the conduction band by appropriate doping emerges as a natural strategy for reinforcing FM interactions and eventually raising T_C for double perovskites. Indeed, it has been shown that replacement in Sr_2FeMoO_6 of divalent Sr^{2+} by trivalent La^{3+} does raise T_C by more than 80 K [3–5]. However, this raising is accompanied by a huge increase in the antisite (AS) defect concentration, which lowers the saturation magnetization [3]. It is thus obvious that other alternatives for electron doping or suppression of antisites should be explored. In that direction, use of Nd^{3+} as a dopant ion in $Sr_{2-x}Nd_xFeMoO_6$ may be doubly interesting. Firstly, it may also act as an electron donor thus eventually giving rise to a T_C enhancement. On the other hand, the Nd^{3+} ion is much smaller than Sr^{2+}, and it could be suspected that this size difference may favour some ordering of the A-site ions (Sr/Nd) and eventually promote some order in the Fe/Mo sublattice, thus reducing the AS defect concentration. Indications for this trend can be derived from the recent finding that AS defects can be largely suppressed in $Sr_{2-x}Ca_xFeMoO_6$ [6].

In this work, we report the results obtained from the study of electron doped (Nd^{3+}) $Sr_{2-x}Nd_xFeMoO_6$ samples. We show that T_C for SFMO is significantly increased by Nd^{3+} substitution as a consequence of band filling effects. Additionally, we provide further evidence about the weak influence of steric effects on the magnetic interactions of SFMO related compounds. We suggest that the increase of the level of AS defects upon doping is intimately related to the valence of the substituting species. Finally, the impact of disorder on the magnetotransport properties of double perovskites is discussed. We argue that the half-metallic ferromagnetic character of double perovskites may be unstable in the presence of AS defects.

2. Experimental details

Ceramic samples of $Sr_{2-x}Nd_xFeMoO_6$ ($0 \leqslant x \leqslant 0.6$) were synthesized by means of standard solid state reactions. High purity oxides (Nd_2O_3, Fe_2O_3, MoO_3) and carbonates ($SrCO_3$) were mixed in the appropriate ratio. The mixtures were calcined twice (with intermediate and final grindings) at 900 °C. After that, powders were pressed into 0.6 g pellets, and synthesized at 1250 °C in a mixture of 1% H_2 in Ar. Finally, samples were slowly cooled down at -1 °C min^{-1}. Two different batches, A and B, with $x = 0$, 0.2, 0.4 and 0.6 and with $x = 0.1$, 0.2 and 0.3 respectively were prepared. Results obtained from batches A and B were revealed to be consistent with each other.

Structural characterization was performed by means of x-ray diffraction (XRD) using a Siemens D-5000 diffractometer and Kα_1, α_2 (Cu) radiation. The diffraction profiles obtained were analysed by means of the Rietveld method using FULLPROF [7] software. All samples turned out to be single phase, with only small traces (<0.5%) of $SrMoO_4$ observed in some cases. It will be useful to recall here some ionic radii values: $r_{Sr^{2+}} = 1.26$ Å, $r_{La^{3+}} = 1.160$ Å, $r_{Ca^{2+}} = 1.12$ Å and $r_{Nd^{3+}} = 1.109$ Å.

Magnetic characterization was done by means of a Quantum Design SQUID magnetometer (2–300 K, up to 5.5 T). Magnetic measurements above room temperature were made using a vibrating sample magnetometer (VSM). Magnetotransport properties were measured in a PPMS system from Quantum Design using the standard four-probe method.

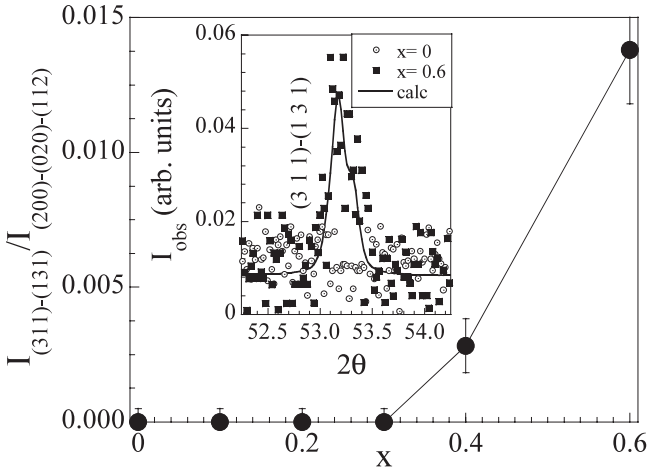

Figure 1. The integrated intensity of the (311)–(131) doublet (forbidden in the $I4/m$ SG) normalized to that of the most intense peak ((200)–(020)–(112) triplet), as a function of the Nd doping level x. The transition to a primitive lattice is evidenced for $x \leqslant 0.4$. The inset shows this doublet in the $x = 0.6$ case, together with the refinement in the $P2_1/n$ SG and the same region in the $x = 0$ case. Notice that the intensity of the (311)–(131) doublet is only about 1% of the intensity of the most intense reflection in SFMO.

The non-doped sample ($x = 0$) obtained showed structural and magnetic properties fully consistent with those reported in [6] for pristine compounds belonging to the $La_xSr_{2-x}FeMoO_6$ and $Ca_xSr_{2-x}FeMoO_6$ series. As neutron powder diffraction revealed than both the $La_xSr_{2-x}FeMoO_6$ and $Ca_xSr_{2-x}FeMoO_6$ series are cation and oxygen stoichiometric [6], we can reasonably assume that the samples reported on in this paper are so too.

3. Results and discussion

3.1. Structural characterization

XRD profiles corresponding to $Sr_{2-x}Nd_xFeMoO_6$ samples with $x < 0.4$ were successfully refined using the tetragonal $I4/m$ space group, as found for Sr_2FeMoO_6 [8]. For $x = 0.4$ and 0.6, diffraction patterns reveal the presence of weak reflections, forbidden in the I centred symmetry, reflecting the lowering of symmetry upon Nd substitution. This can be followed in figure 1, where we show the evolution of the integrated intensity of the (311)–(131) doublet, not permitted in a body centred space group. A detail of the diffracted patterns for the $x = 0$ and 0.6 samples around $2\theta \approx 53^\circ$ can also be seen in figure 1 (inset), evidencing the appearance of the (311)–(131) doublet. The smaller size of the substituting Nd ions implies a progressive tilting and rotation of the oxygen octahedral driving the symmetry reduction. Accordingly, we have refined the XRD patterns of the $x = 0.4$ and 0.6 samples using the monoclinic $P2_1/n$ space group, as found in La doped $Sr_{2-x}La_xFeMoO_6$ [3] or Ca_2FeMoO_6 [9].

The evolutions of lattice parameters and the cell volume with doping (x) are depicted in figures 2(a) and (b). Data in figure 2(a) show a non-monotonic evolution of lattice parameters with doping, which reflects the change of symmetry. A more striking result is the observation that the unit cell volume (solid and open triangles in figure 2(b)) remains almost constant upon Nd doping. This effect results from the competition (and compensation) of two opposite effects: a steric one, promoting a volume contraction due to the smaller ionic radii of Nd^{3+} with

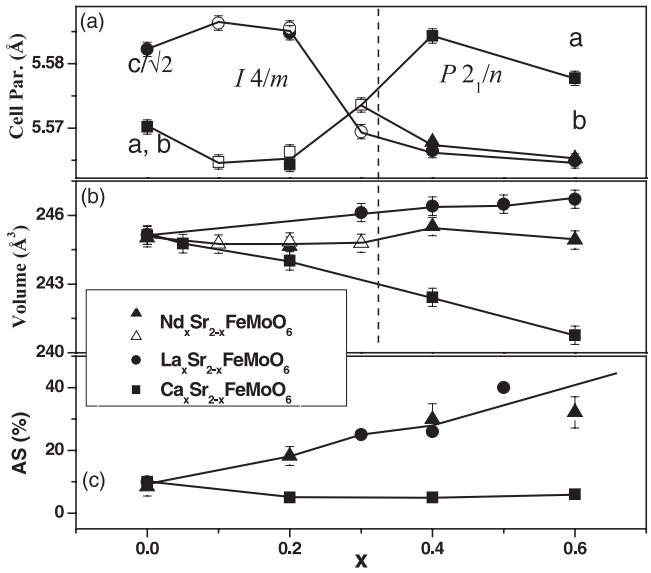

Figure 2. (a) Cell parameters as a function of Nd doping. The dashed line indicates the structural transition from $I4/m$ to $P2_1/n$. Filled symbols indicate samples belonging to batch A, while open symbols correspond to batch B samples. (b) Evolution of the cell volume with doping for Nd, La and Ca doped samples. Connecting lines are guides for the eye. Data for La and Ca doped samples are taken from [6] and [10]. (c) Antisite concentration (AS) as a function of doping, for Nd (the error bars are indicated), La and Ca doped samples (from [6]). Connecting lines are guides for the eye.

respect Sr^{2+}, and an electronic effect, which results from the (Fe, Mo)–O bond expansion due to the electron filling of antibonding states of SFMO. It is interesting to compare this results with those obtained from the study of $Sr_{2-x}Ca_xFeMoO_6$ [10] and $Sr_{2-x}La_xFeMoO_6$ [6] series. These data are also included in figure 2(b). The Ca^{2+} doped series shows a volume contraction due exclusively to the contribution of the ionic size effects (Ca^{2+} is isovalent but smaller than Sr^{2+}), while the La^{3+} doped samples show a slight cell expansion, attributable to the electronic effect overcoming the structural one (as $r_{Nd^{3+}} < r_{La^{3+}} < r_{Sr^{2+}}$, the steric effect in this series should be weaker than in the case of Nd^{3+} substitution).

The concentration of AS defects is defined as the fraction of Fe (Mo) ions misplaced at Mo (Fe) sites. Under this convention, 50% AS means a completely disordered Fe–Mo sublattice. The AS concentration of each sample was determined from the refinement of XRD patterns. Figure 2(c) (solid triangles) shows the evolution of AS in Nd doped samples, revealing a large increase in AS concentration upon Nd substitution. Incidentally it is worth recalling that the integrated intensity of the superstructure reflection associated with the ordering of the Fe/Mo sublattice is not sensitive to antiphase boundaries [11], although the contribution of these extended defects is clearly visible through the enhanced broadening of the superstructure reflection. We have also included in figure 2(c) the measured AS concentration for La^{3+} (solid circles) [6] and Ca^{2+} (solid squares) [6] substituted samples. From inspection of the data in figure 2(c) one immediately recognizes that the change in AS disorder in doped Sr_2FeMoO_6 samples is not controlled by the size of the dopant ion (as $r_{Nd^{3+}} < r_{Ca^{2+}} < r_{La^{3+}}$), but by its valence. It is well known that the order of the B/B′ sublattice decreases on decreasing the charge difference between B and B′ cations. Under these circumstances, the enhancement of the cationic disorder upon electron doping can be viewed as a consequence of the selective

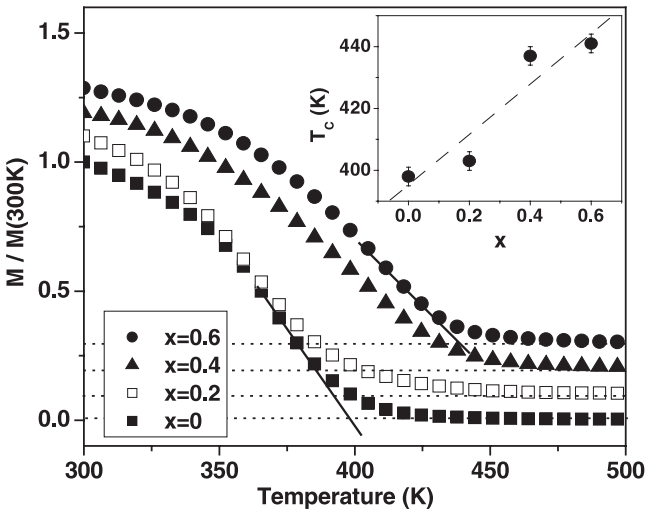

Figure 3. Main panel: temperature dependent magnetization (measured at 1 kOe) for $Nd_xSr_{2-x}FeMoO_6$ samples. Curie temperatures were determined from the extrapolation of the transition region (straight lines) to the zero-magnetization level (dashed lines). Curves were normalized at 300 K, and shifted up in order to clarify the picture. Inset: the evolution of the Curie temperature (T_C) for the Nd doped $Nd_xSr_{2-x}FeMoO_6$ series.

localization of injected electrons on Mo sites, as inferred from neutron powder diffraction [6], nuclear magnetic resonance [12] and Mössbauer [13] experiments. This produces a decrease of the Mo valence from Mo^{6+} towards Mo^{5+}, while the Fe^{2+} charge state remains nearly invariant; accordingly the charge difference between Fe and Mo ions is reduced and thus the driving force for Fe/Mo ordering becomes weaker. It is worth mentioning that recent NMR experiments [12] have shown that the presence of AS disorder does not produce any appreciable variation in the charge state of Mo ions and thus it can be concluded that the presence of Mo–O–Mo bonds (induced by AS defects) does not promote significant charge localization on Mo sites. Therefore, the observed variation of the Mo valence upon doping [12] must be unambiguously attributed to electron doping.

3.2. Magnetic behaviour

Figure 3 shows the evolution of the magnetization with temperature. All curves were normalized at 300 K and shifted up, for the sake of clarity. Dotted lines indicate the zero-magnetization level for each case. Curie temperatures were determined from the extrapolation of the magnetization in the transition region to zero magnetization, as indicated by solid lines through some data in figure 3. This figure evidences that T_C rises upon Nd doping. It is particularly relevant that for $x = 0.6$, T_C increases to as much as ∼40 K above that of the pristine compound. The T_C extracted as a function of Nd contents are shown in figure 3 (inset). Assuming a roughly linear dependence of T_C on x, and performing a linear fit, an increase rate (dT_C/dx) of about 1.6 K/(% of Nd) is found. We note that this dT_C/dx value is comparable with 1.3 K/(% of La) reported for $La_xSr_{2-x}FeMoO_6$ samples [3]. It is worth recalling that this reinforcement of the magnetic interactions upon electron doping in the $La_xSr_{2-x}FeMoO_6$ series was also confirmed using alternative experimental tools such as Arrott plots [4] and neutron diffraction [6]. Similarly, for the partially Ba substituted $(Ba_{0.8}Sr_{0.2})_{2-x}La_xFeMoO_6$ series, neutron diffraction experiments also confirmed that La substitution promotes a similar effect [5]. Although certainly the precise value of T_C and the corresponding ratio dT_C/dx may

depend on the technique involved in the determination of T_C, the experimental data shown in figure 3 unambiguously indicate a very significant augmentation of T_C upon Nd substitution.

Returning to the previous comparison between Nd and La doped samples, and bearing in mind their different structural properties (as discussed above), the similar rises in T_C for the two sets of samples supports the idea that the magnetic interactions in double perovskites are not strongly correlated with small structural variations. In consequence, we should conclude that the observed increment of T_C upon electronic doping is mainly due to band filling effects. This is also consistent with recent NPD experiments on $La_xSr_{2-x}FeMoO_6$ and $Ca_xSr_{2-x}FeMoO_6$ samples [6], where it was found that the relation between the strength of the magnetic interactions (i.e. the value of T_C) and the evolution of the Fe–O–Mo bond angle is much smaller than that found in manganites [14]. A key point for understanding this dissimilarity in behaviour is that the electrons involved in the magnetic interactions of double perovskites are of (Fe, Mo) d t_{2g} parentage, while in the case of manganites they are of (Mn) d e_g parentage. As the angular dependence of the matrix elements describing the orbital hybridization (and thus the band formation) depends on the symmetry of the particular orbitals involved, different angular dependences must be expected between t_{2g} (pointing in between surrounding oxygen ions) and e_g (pointing directly to the surrounding oxygen ions) orbitals. Indeed, the bandwidth of Mn perovskites is known to depend critically on the Mn–O–Mn bond angles (in other words, the e_g–O_{2p}–e_g orbital overlap is severely affected by bond bending) whereas a weaker dependence of the t_{2g}–O_{2p}–t_{2g} overlap on the bond angle can be anticipated. Our results suggest that in the case of double perovskites the above mentioned overlapping is indeed weakly affected by structural modifications.

Isothermal magnetization versus field data (taken at 10 K) are shown in figure 4(a). In the first place, we notice that the magnetization of the samples is reduced as the Nd concentration increases. This point, intimately related to the increase in AS defect level when Nd is introduced into the structure, will be discussed in detail below. Data in figure 4(a) also show that, with the exception of the $x = 0$ sample case, the high field magnetization does not saturate. A differential susceptibility (χ_d) is clearly manifested by the linear increase of the magnetization $M(H)$ in the high field region. Inspection of data in figure 4 immediately reveals that χ_d augments with the Nd^{3+} content of the samples, as depicted in figure 4(b) (inset), where a clear linear dependence on the Nd concentration is seen. There are two contributions to the high field susceptibility: the first one comes from the magnetic hardening of the material due to the presence of antisites (χ_d^{AS} (AS)), as reported in [15]; the second one is due to the magnetic contribution of paramagnetic Nd^{3+} ions ($\chi_d^{Nd^{3+}}(x)$). Assuming that the Nd^{3+} contribution is the dominant one and neglecting any magnetic interaction between Nd^{3+} ions and the Fe–Mo sublattice, the effective moment μ_{eff} of Nd^{3+} ions can be roughly estimated assuming that the paramagnetic Nd^{3+} follows a Curie law:

$$\chi_d(x) \approx \chi_d^{Nd^{3+}} = x\mu_{eff}^2/3\,k_B T$$

where χ is the paramagnetic susceptibility per unit cell. From the slope of $\chi_d^{Nd^{3+}}(x)$ data we obtain a value of $\mu_{eff}(Nd^{3+}) \cong 2.85\ \mu_B$. This value is intermediate between those reported for the perovskites $Nd_{0.7}A_{0.3}MnO_3$ (A = Ca, Sr, Ba, Pb) ($\mu_{eff}(Nd^{3+}) = 0.3$–$0.9\ \mu_B$) [16] and $NdGaO_3$ ($\mu_{eff}(Nd^{3+}) \cong 3.95\ \mu_B$) [17]. Figure 4(a) also shows (as dashed lines) the magnetization obtained after subtraction of the paramagnetic contribution of the Nd^{3+} ions. Corrected saturation magnetization values (M_S^c) are depicted in figure 4(b) (solid symbols). Data in this figure evidence that M_S^c decays rapidly upon Nd doping, in much the same way as reported earlier for La doped SFMO [3]. As described in [3], it is possible to estimate the saturation magnetization by means of the simple model

$$M_S(AS, x) = 4(1 - 2AS)\mu_B - x(1 - 2AS)\mu_B$$

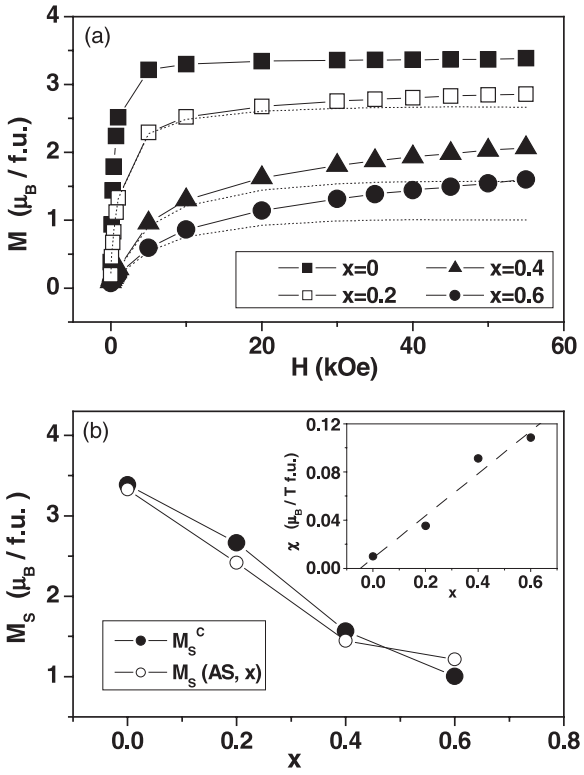

Figure 4. (a) Magnetization curves (10 K) for samples of the $Nd_xSr_{2-x}FeMoO_6$ series. Dashed lines show corrected magnetization curves after subtracting the paramagnetic contribution of Nd^{3+}, as explained in the text. (b) Saturation magnetization M_S^c (obtained after subtracting the Nd^{3+} contribution) values as a function of Nd content (solid symbols). The values of M_S (AS, x), as defined in the text, are also shown (open symbols). The inset shows the evolution of the high field differential susceptibility with Nd doping.

where the first term corresponds to the decrease of magnetization due to the presence of AS defects [18], while the second one takes into account the reduction of magnetization due to the injection of electrons—by doping—on the 'spin down' band [3]. The calculated M_S (AS, x) values, included also in figure 4(b), reproduce quite accurately the experimental ones. We thus conclude that in Nd doped samples, the reduction of magnetization upon Nd substitution can be well described by the combined effect of AS and electron injection into the spin down band.

3.3. Transport properties

The temperature dependence of the normalized resistivity is shown in figure 5. All the curves were normalized by the corresponding resistivity values at 300 K, which vary between 0.5 and 5 mΩ cm for the whole series, as shown in the inset of figure 5. The low values of the measured resistivity suggest the presence of intrinsic metallic conduction paths somewhat modified by intergranular contributions, unavoidable in these measurements on ceramic samples. It is worth recalling that resistivity measurements on Sr_2FeMoO_6 single crystals and epitaxial thin films show metallic behaviour and typical resistivity values of ∼0.4 mΩ cm [19] and ∼1 mΩ cm [20], respectively. In consequence, the very slightly negative temperature

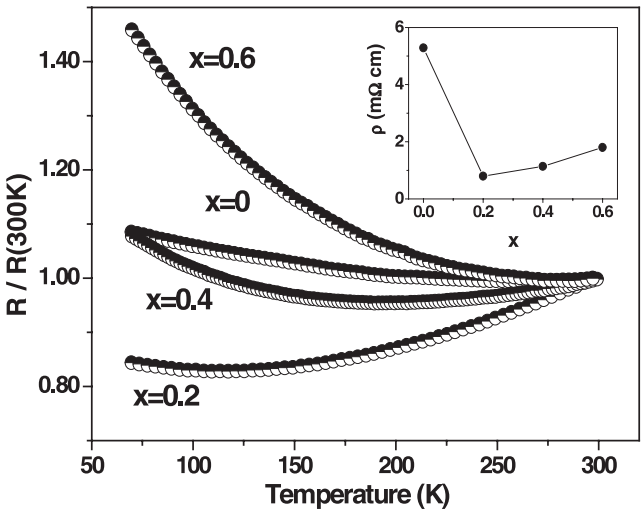

Figure 5. Main panel: evolution of the resistivity with temperature, for $Nd_xSr_{2-x}FeMoO_6$ samples. All curves were normalized at 300 K. Inset: room temperature resistivity values for Nd doped samples.

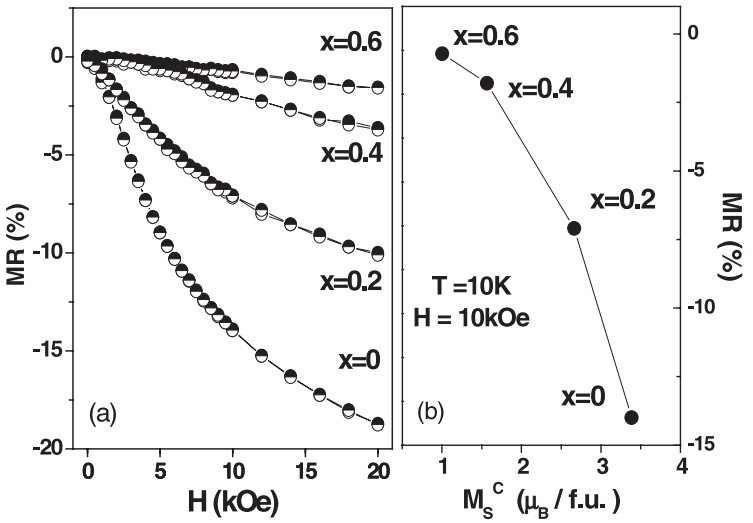

Figure 6. (a) The low temperature (10 K) magnetoresistance, up to 20 kOe, of Nd doped samples. The magnetoresistance (MR) is defined as $[R(H) - R(H = 0)/R(H = 0)]$. (b) MR values (extracted at 10 kOe) as a function of the corrected saturation magnetization (M_S^c), for $Nd_xSr_{2-x}FeMoO_6$ samples.

coefficients seen for some of our samples will be attributed to the above mentioned grain boundary contribution, while the resistivity values suggest that the bulk conductivity remains essentially metallic upon Nd substitution.

Figure 6(a) shows the low temperature (10 K) magnetoresistance (MR), measured under fields up to 20 kOe. We must recall that MR in SFMO and related oxides is thought to be caused by an intergranular magnetic tunnelling process, which is mainly determined by the high spin polarization of conduction electrons. It is clear from figure 6(a) that MR decays

rapidly upon Nd doping. Moreover, figure 6(b) shows that this fall in MR is concomitant with the reduction in saturation magnetization (M_S) with Nd content. If a rigid band model is assumed (which implies that the band structure remains unmodified upon Nd doping), the half-metallic character of DP (and therefore any tunnel magnetoresistance) should not be affected when injecting electrons in the conduction band. Hence, our experimental data could be an indication that the severe increase in the level of AS defects upon Nd doping may produce a suppression of the half-metallic ferromagnetic behaviour. This result can be expected from considering that misplaced Fe^{3+} ions couple antiferromagnetically to Fe^{3+} near neighbours and thus introduce carriers and electronic states of opposite spin polarity in the conduction band. A similar behaviour may be expected in the case of carriers belonging to misplaced Mo ions. Under these circumstances, the presence of AS defects will suppress the half-metallic ferromagnetic character of double perovskites. From recent photoemission experiments, indeed, it was concluded that a rigid band model cannot account for the measured spectroscopic data on La substituted samples [21]. Moreover, recent *ab initio* calculations, reported by Sarma and Saha-Dasgupta [22], also suggest that disorder effects should destroy the half-metallic ferromagnetic state of SFMO.

4. Summary and conclusions

In summary, we have reported on the structural, magnetic and transport properties promoted by Nd^{3+} substitution in the $Sr_{2-x}Nd_xFeMoO_6$ series. We have found that, although the ionic size of the Nd^{3+} ion is smaller than that of the Sr^{2+} ion, this cationic substitution does not produce a modification of the unit cell volume. This is interpreted as a manifestation of the competitive effects of bond expansion due to the injection of doping electrons into empty Fe–O–Mo based orbitals and steric effects. This striking observation contrasts with the finding that the ferromagnetic Curie temperature rises at a rate of $dT_C/dx \approx 1.6$ K/(% of Nd) and demonstrates that the reinforcement of the ferromagnetic interactions in double perovskites is a genuine electronic effect. However, we have also found that, accompanying the electron doping, the concentration of disordered Fe(Mo) at Mo(Fe) sites also increases. From the comparison of the concentration of AS defects promoted by partial replacement of Sr^{2+} ions by heterovalent (such as Nd^{3+} or La^{3+}) or isovalent (Ca^{2+}) ions, we conclude that the electron donor character of the substitutional ions, rather than the size, largely determines the AS concentration. Of great relevance is the finding that AS defects simultaneously reduce the saturation magnetization *and* the magnetoresistance of the samples. We have argued that this observation could imply that the energy gap between spin up and spin down sub-bands may be closed, and consequently the half-metallic ferromagnetic character of double perovskite may be lost in the presence of AS defects. As this result may represent a severe restriction on practical applications in magnetoelectronic devices, the development of strategies for raising the Curie temperature of SFMO while the AS concentration remains low is needed.

After the completion of this paper, a report [13] exploring the effects of Nd doping in Sr_2FeMoO_6 has been published. Consistently with our results, it is found that the Curie temperature is pushed up upon Nd substitution, and selective doping on the Mo site is suggested.

Acknowledgments

We thank the AMORE (CEE), MAT 1999-0984-C03, MAT 2002-03431 and MAT 2003-07483-C02-02 projects for financial support. CF thanks for financial support the MCyT (Spain).

References

[1] Kobayashi K I, Kimura T, Sawada H, Terakura K and Tokura Y 1998 *Nature* **395** 677
[2] Tovar M, Causa M T, Butera A, Navarro J, Martinez B, Fontcuberta J and Passeggi M C G 2002 *Phys. Rev.* B **66** 024409
[3] Navarro J, Frontera C, Balcells L l, Martinez B and Fontcuberta J 2001 *Phys. Rev.* B **64** 092411
[4] Navarro J, Nogués J, Muñoz J S and Fontcuberta J 2003 *Phys. Rev.* B **67** 174416
[5] Serrate D, De Teresa J M, Blasco J, Ibarra M R and Morellón L 2002 *Appl. Phys. Lett.* **80** 24
[6] Frontera C, Rubi D, Navarro J, García-Muñoz J L, Fontcuberta J and Ritter C 2003 *Phys. Rev.* B **68** 012412
[7] Rodríguez Carvajal J 1993 *Physica* B **192** 55
[8] Sánchez D, Alonso J A, García-Hernández M, Martínez López M J, Martínez J L and Mellergard A 2002 *Phys. Rev.* B **65** 104426
[9] Alonso J A, Casais M T, Martínez-Lopez M J, Martínez J L, Velasco P, Muñoz A and Fernández-Díaz M T 2000 *Chem. Mater.* **12** 161
[10] Ritter C, Rubi D, Navarro J, Frontera C, García-Muñoz J L and Fontcuberta J 2004 *J. Magn. Magn. Mater.* at press
[11] Warren B E 1980 *X-Ray Diffraction* (New York: Dover)
[12] Wojcik M, Jedryka E, Nadolski S, Navarro J, Rubi D and Fontcuberta J 2004 *Phys. Rev.* B **69** 100407(RC)
Wojcik M, Jedryka E, Nadolski S, Navarro J, Rubi D and Fontcuberta J 2003 *Preprint* cond-mat/0310689
[13] Lindén J, Shimada T, Motohashi T, Yamauchi H and Karppinen M 2004 *Solid State Commun.* **129** 129–33
[14] Fontcuberta J, Martinez B, Seffar A, Piñol S, García-Muñoz J L and Obradors X 1996 *Phys. Rev. Lett.* **76** 1122
[15] Navarro J, Balcells L l, Sandiumenge F, Bibes M, Roig A, Martinez B and Fontcuberta J 2001 *J. Phys.: Condens. Matter* **13** 8481–8
[16] Thomas R-M, Skumryev V and Coey J M D 1999 *J. Appl. Phys.* **85** 8
[17] Podlesnyak A, Rosenkranz S, Fauth F, Marti W, Furrer A, Mirmelstein A and Scheel H J 1993 *J. Phys.: Condens. Matter* **5** 8973–82
[18] Balcells L l, Navarro J, Bibes M, Roig A, Martinez B and Fontcuberta J 2001 *Appl. Phys. Lett.* **78** 781
[19] Tomioka Y, Okuda T, Okimoto Y, Kumai R, Kobayashi K-I and Tokura Y 2000 *Phys. Rev.* B **61** 422
[20] Manako T, Izumi M, Konishi Y, Kobayashi K-I, Kawasaki M and Tokura Y 1999 *Appl. Phys. Lett.* **74** 2215
[21] Navarro J, Fontcuberta J, Izquierdo M, Avila J and Asensio M C 2003 *Preprint* cond-mat/0303464
[22] Saha-Dasgupta T and Sarma D D 2001 *Phys. Rev.* B **64** 064408